nature geoscience

LETTERS

PUBLISHED ONLINE: 27 OCTOBER 2013 | DOI: 10.1038/NGEO1982

Ponded melt at the boundary between the lithosphere and asthenosphere

Tatsuya Sakamaki[1]*, Akio Suzuki[1], Eiji Ohtani[1], Hidenori Terasaki[2], Satoru Urakawa[3], Yoshinori Katayama[4], Ken-ichi Funakoshi[5], Yanbin Wang[6], John W. Hernlund[7†] and Maxim D. Ballmer[8]

The boundary between Earth's rigid lithosphere and the underlying, ductile asthenosphere is marked by a distinct seismic discontinuity[1]. A decrease in seismic-wave velocity and increase in attenuation at this boundary is thought to be caused by partial melt[2]. The density and viscosity of basaltic magma, linked to the atomic structure[3,4], control the process of melt separation from the surrounding mantle rocks[5–9]. Here we use high-pressure and high-temperature experiments and *in situ* X-ray analysis to assess the properties of basaltic magmas under pressures of up to 5.5 GPa. We find that the magmas rapidly become denser with increasing pressure and show a viscosity minimum near 4 GPa. Magma mobility—the ratio of the melt–solid density contrast to the magma viscosity—exhibits a peak at pressures corresponding to depths of 120–150 km, within the asthenosphere, up to an order of magnitude greater than pressures corresponding to the deeper mantle and shallower lithosphere. Melts are therefore expected to rapidly migrate out of the asthenosphere. The diminishing mobility of magma in Earth's asthenosphere as the melts ascend could lead to excessive melt accumulation at depths of 80–100 km, at the lithosphere–asthenosphere boundary. We conclude that the observed seismic discontinuity at the lithosphere–asthenosphere boundary records this accumulation of melt.

Along the axial zone of mid-ocean ridges (MORs), asthenospheric mantle rises in response to the diverging motion of oceanic lithosphere and experiences decompression melting. Depending on the volatile content and temperature of the upper mantle, peridotite partial melting initiates at depths of about 80–130 km (ref. 10). The resulting basaltic magmas are buoyant and mobile, percolating upward to form the crust, and leaving a refractory residuum that forms the oceanic lithosphere. Along the more than 50,000-km-long global MOR system, roughly 60,000 tons of magma are processed per minute[11], replenishing the entire ocean floor in ~100 Myr. This process is the primary engine for present-day geochemical fractionation of our planet.

Structural changes in basaltic magmas with pressure (or depth) play a central role in controlling magma mobility and melting. Pressure-dependent structural changes in silicate melts associated with transformations in the coordination of aluminium ions have been suggested from nuclear magnetic resonance spectroscopic studies of quenched glasses[3]. Such structural changes usually influence physical properties such as density and viscosity of magmas. Density measurements of basaltic magmas have thus far been carried out using the sink–float method[5,6], which is subject to large uncertainties. Here, we use X-ray absorption[12,13], an alternative method that enables determination of liquid density *in situ* (that is, under ambient pressure and temperature conditions). Furthermore, we apply *in situ* falling-sphere viscometry and *in situ* X-ray diffraction to measure magma viscosity and magma structure, respectively. The resulting complete and detailed data set allows us to examine pressure-dependent changes of magma density, viscosity and structure in unprecedented detail.

X-ray absorption measurements were performed up to 4.5 GPa and 2,000 K (Fig. 1a). The composition of the starting materials is shown in Supplementary Table 1 and the experimental results on density are summarized in Fig. 1a and Supplementary Table 2. In Fig. 1b, we compile available data from refs. 5,6,14 to compare with our results at 2,000 K. We find that density of basaltic magmas increases rapidly at pressures of ~4 GPa. Such rapid densification is consistent with previous studies on quenched alumino-silicate melts, which showed that Al coordination number increases rapidly between 3 and 5 GPa (ref. 3).

We further conducted *in situ* viscosity measurements using the falling-sphere method with X-ray radiography[7] (Fig. 1c and Supplementary Table 3). Figure 1c summarizes our results and gives the viscosities of abyssal tholeiite magma at 0.8 and 1.2 GPa (ref. 9) for reference. For basaltic magma, the isothermal viscosity first decreases and then increases with pressure. Viscosity minima are clearly discernible, both along the 1,900 and 2,000 K isotherms (Fig. 1c). The pressure of the viscosity minimum further coincides with that of rapid densification, suggesting that both are related to the same pressure-induced structural changes in the basaltic magma.

To clarify the nature of the structural changes we performed X-ray diffraction experiments from 1.9 to 5.5 GPa at 1,800–2,000 K. The experimental conditions and results are reported in the Supplementary Methods and Table 4[4,15,16]. The X-ray diffraction interference functions, $Qi(Q)s$, as calculated for the basaltic magma, are shown in Supplementary Fig. 3a, and its Fourier transform $G(r)$, that is, the radial distribution function, in Supplementary Fig. 3b. The first peak at $r = 1.6$–1.7 Å corresponds to the average T–O bond

[1]Department of Earth and Planetary Materials Science, Tohoku University, Sendai 980-8578, Japan, [2]Department of Earth and Space Science, Osaka University, Osaka 560-0043, Japan, [3]Department of Earth Sciences, Okayama University, Okayama 700-8530, Japan, [4]Japan Atomic Energy Agency, Hyogo 679-5148, Japan, [5]SPring-8, Japan Synchrotron Radiation Research Institute, Hyogo 679-5198, Japan, [6]Center for Advanced Radiation Sources, The University of Chicago, Chicago, Illinois 60637, USA, [7]Department of Earth and Planetary Science, University of California, Berkeley 94720, USA, [8]Department of Geology and Geophysics, School of Ocean and Earth Sciences and Technology, University of Hawaii at Manoa, Honolulu, Hawaii 96822, USA. †Present address: Earth-Life Science Institute, Tokyo Institute of Technology, Meguro-ku, Tokyo 152-8550, Japan. *e-mail: sakamaki@m.tohoku.ac.jp

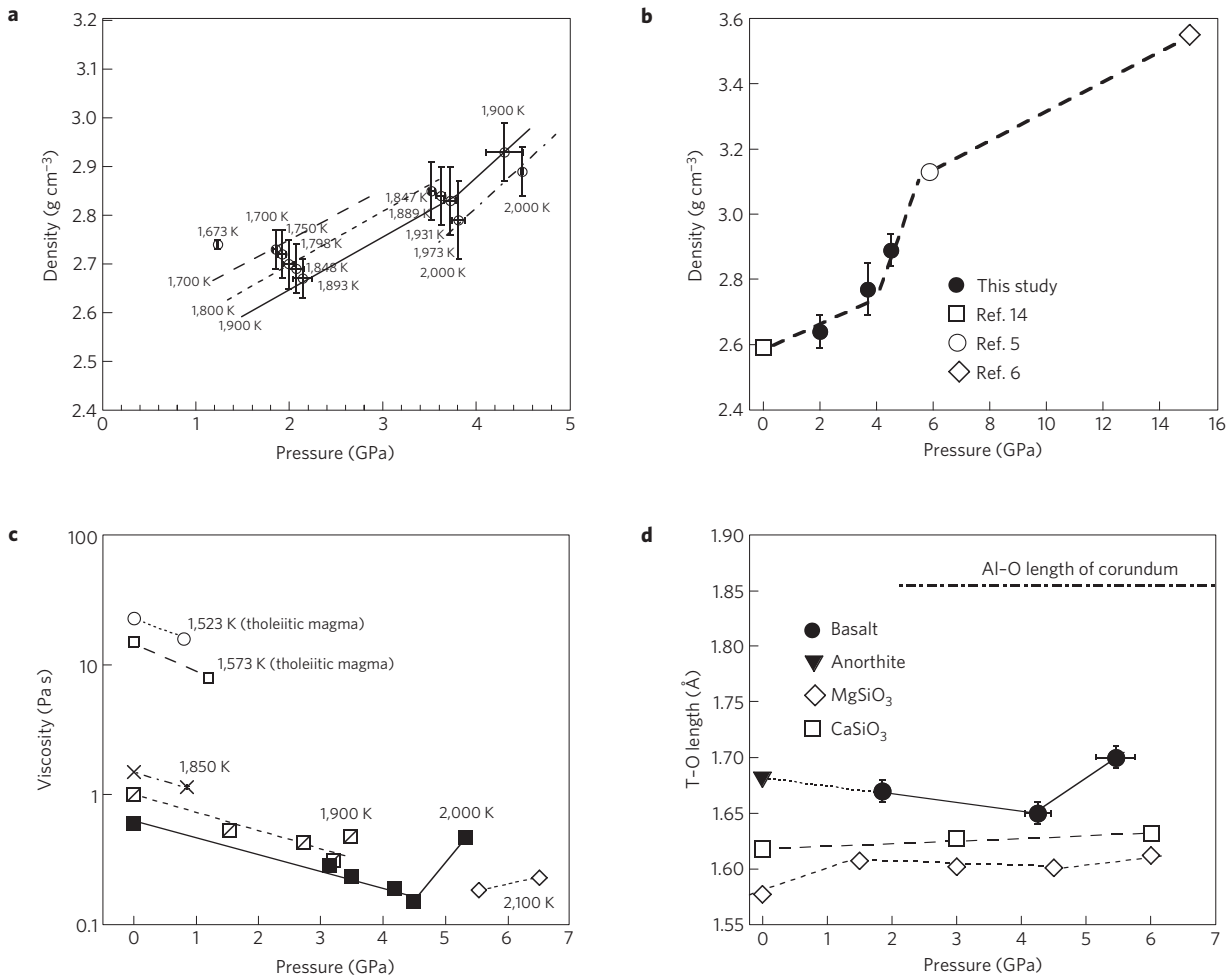

Figure 1 | Results of the experimental study. a, Density of basaltic magma as a function of pressure and temperature. **b**, Density of basaltic magma as a function of pressure at 2,000 K. Anomalous densification occurs between 4 and 6 GPa. **c**, Viscosity of basaltic magma at high pressure and temperature. Error bars are smaller than symbols. **d**, Pressure dependence of the T–O bond length of basaltic magma from this study, and other silicate melts from previous studies. Al–O bond length of corundum is shown for comparison[30].

length, that is, the length between tetrahedrally coordinated cations ($T = Si^{4+}$, Al^{3+}) and oxygen.

The T–O bond length is a characteristic parameter of the network structure of magmas. Figure 1d compares the T–O length of basaltic magma as a function of pressure with those of $MgSiO_3$ and $CaSiO_3$ melts, and corundum. No experimental data for the structure of basaltic magma at ambient pressure are available for benchmark. For reference, we use the T–O length of anorthite melt at zero pressure[16]. The T–O bond length in basaltic magma at ambient pressure may be shorter than that of anorthite melt owing to less Al_2O_3 component. We find that, for basaltic melt, the T–O length decreases between 1.9 and 4.3 GPa, and then increases between 4.3 and 5.5 GPa. Only the initial decrease is consistent with simple compression of the magma. As the T–O lengths in TO_6 octahedra are generally longer than those of TO_4 tetrahedra[17], the extension of the T–O length at high pressures is consistent with an increase in cation coordination. Between 4 and 6 GPa, the increase of Al^{3+} coordination is generally more extensive than that of Si^{4+} (ref. 3). Therefore, the rapid density increase of basaltic magma at these pressures is attributed to an increase in Al^{3+} coordination. This behaviour is singular compared with other silicic melts: T–O lengths have been reported to only modestly increase with pressure for $MgSiO_3$ and $CaSiO_3$ melts[4,15] (Fig. 1d).

Basaltic magmas formed by deep small-extent melting (>120 km depth) may be stabilized by volatiles such as CO_2[10]. Although the effect of CO_2 on melt viscosity above 2.5 GPa is unknown at present, according to ref. 18, for $NaCaAlSi_2O_7$ and albite melts, CO_2 reduces the viscosity slightly, but the pressure of the viscosity minimum remains unchanged; that is, the viscosity minimum for basaltic magmas should persist at ~120 km. The effect of CO_2 on magma density is also insignificant, that is, less than 1% when 1 wt% CO_2 dissolves in the melt[13]. The water concentration of normal MOR basalts is 0.07–0.19 wt% and their source mantle contains 330 ppm H_2O (refs 19,20). Although H_2O affects the viscosity and density of the magmas[21], we can ignore the effect of H_2O in magmas containing this small amount of H_2O.

Gravity-driven separation of buoyant magma from partially molten rock is proportional to the hydrostatic magma mobility (defined as $\Delta\rho/\eta$) in addition to the permeability[22]. Here, η is melt viscosity, and $\Delta\rho$ is the density difference between the magma and the surrounding solid rock (for which we take olivine Fo_{90} (ref. 23) as representative). Figure 2a shows that, for any plausible choice of geotherm (see Supplementary Information), $\Delta\rho$ decreases rapidly from 100 to 180 km depth (that is, ~3.5 to ~6 GPa). This transition is caused by a coordination change of Al in the melt with an unusually large compressibility almost five times higher than usual above and below this depth range. In addition, $\Delta\rho$ slightly decreases from ~100 km depth to the surface (Fig. 2a). This slight decrease of $\Delta\rho$ is a conservative estimate as we do not consider the effects of successive removal of garnet and clinopyroxene, as well

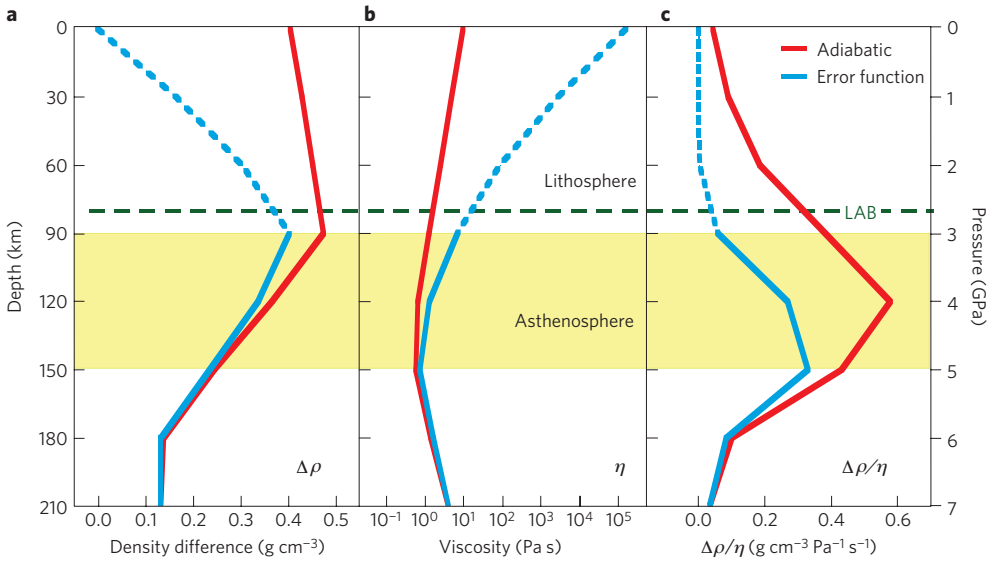

Figure 2 | Magma properties and mobility as a function of depth. a, Density difference between basaltic magma and olivine ($\Delta\rho$) as a function of depth (and pressure). The red and blue lines are based on an adiabatic temperature gradient, and a realistic error-function temperature profile for mature oceanic lithosphere, respectively. The potential temperature is 1,623 K. Yellow shading highlights the depth range with anomalous physical properties of basaltic melts due to the structural transition in Al coordination. **b**, Viscosity (η) of basaltic magma along the same two profiles. Hypothetical subsolidus density and viscosity profiles are dashed. **c**, Mobility $\Delta\rho/\eta$ of basaltic magma along the same two profiles, respectively.

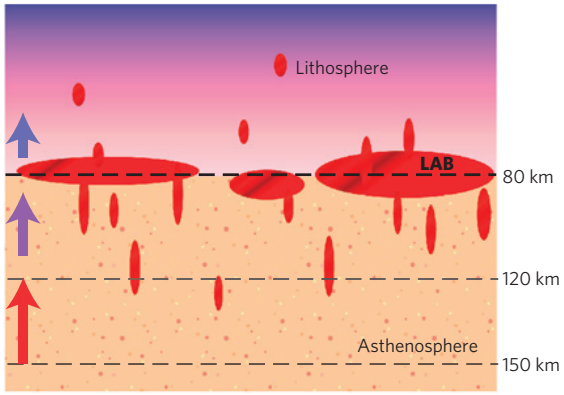

Figure 3 | Schematic illustration of the lithosphere and asthenosphere boundary. Magma mobility is faster between 120 and 150 km, causing relative magma depletion. The lithosphere–asthenosphere boundary (LAB), at around 80 km depth, can be a zone of excessive melt accumulation, because melt can be fluxed at higher rates from below where mobility is higher, but is removed at much slower rates above where mobility is lower.

as of an increase in Mg number (in olivine) in the residual MOR melting column (that is, the oceanic lithosphere). The resulting maximum in $\Delta\rho$ at 3–4 GPa, in combination with a minimum in η at 4–5 GPa (Fig. 2b), results in a peak in magma mobility at ~120–150 km depth in the Earth's mantle (Fig. 2c).

The peak in melt mobility at ~120–150 km depth carries important implications for the nature of Earth's shallow mantle. The decreased mobility of melt as magma ascends from a partially molten asthenosphere gives rise to a tendency for excess melt accumulation at 80–100 km depth (Fig. 3). Unless vertical dykes or channels form in the lithosphere that would otherwise allow the melts to escape[24], magma generated at depth would accumulate atop the asthenosphere. Indeed, a recent magnetotelluric study suggests such a scenario beneath the edge of the Cocos Plate[25]. Excessive melt accumulation at these depths may also lead to rheological weakening, enhanced shear deformation, and formation of sub-horizontal melt bands that would further decrease vertical melt mobility[26–28]. However, this excess magma may also be cooled by heat conduction to the overlying lithosphere, which would cause it to freeze, further restricting permeability and possibly giving rise to the formation of an extensive network of basaltic sills at the base of the lithosphere. Excess melt accumulation at 80–100 km depth may help explain the origin of the seismically observed Gutenberg discontinuity[1], as well as its geographical correlation with features suggestive of recent partial melting of the mantle[2].

Whereas seismically observed low velocities in Earth's asthenosphere have usually been considered as evidence for the presence of retained melt, our results imply that melt mobility is strongly enhanced, which would encourage melt to migrate out of the asthenosphere. Thus, our results might be considered paradoxical unless another mechanism besides partial melt could explain the seismic characteristics of the asthenosphere. One possible resolution is a recent model proposed by in ref. 29, in which the unique seismic properties of the asthenosphere might be accounted for by anelasticity due to grain-boundary sliding, and thus do not require the presence of partial melt. However, this mechanism remains to be tested, and it is unknown whether it can overcome the effects of melt depletion that would be caused by enhanced melt mobility.

Methods

Density of basaltic magmas was measured using the X-ray absorption technique in a DIA-type cubic press at BL22XU of SPring-8. The basaltic sample was compressed at room temperature to the desired pressure, and then melted by resistive heating with a graphite heater. Intensities of the incident and transmitted X-rays (monochromatized at 23 keV) were measured using two ion chambers, located in front and behind the press, respectively, traversing the sample diameter horizontally. Density was calculated according to the Lambert–Beer law. *In situ* X-ray falling-sphere viscometry and structural measurement of basaltic magma were carried out using a Kawai-type multi-anvil apparatus at the BL04B1 of SPring-8. X-ray shadow images of the probing sphere were continuously recorded using a CCD (charge-coupled device) camera with a YAG:Ce fluorescence screen. Magma viscosity was determined on the basis of the terminal velocity of the falling sphere in the molten sample, by analysing recorded image videos. Viscosity of the melt was calculated using the Stokes equation with the Faxén correction for wall effects. Structure of the melt was measured by the multi-angle energy-dispersive

X-ray diffraction method, using a pure Ge solid-state detector. Diffraction patterns were collected at 8 fixed diffraction angles ($2\theta = 4°$, 5°, 7°, 9°, 11°, 15°, 18°, 22°) to cover a wide range of scattering vectors (**Q**). Interference functions and structure factors were calculated using the scattering intensity and atomic scattering factors. Radial distribution functions were obtained by taking Fourier transforms of the interference functions. The peak position was obtained by Gaussian fitting of the peaks.

Received 4 March 2013; accepted 11 September 2013; published online 27 October 2013

References

1. Gutenberg, B. Untersuchungen zur Frage, bis zu welcher Tiefe die Erde kristallin ist. *Z. Geophys.* **2,** 24–29 (1926).
2. Schmerr, N. The gutenberg discontinuity: melt at the lithosphere–asthenosphere boundary. *Science* **335,** 1480–1483 (2012).
3. Allwardt, J. R. *et al.* Effect of structural transitions on properties of high–pressure silicate melts: ^{27}Al NMR, glass densities, and melt viscosities. *Am. Mineral.* **92,** 1093–1104 (2007).
4. Waseda, Y. & Toguri, J. M. in *Dynamic Process of Material Transport and Transformation in the Earth's Interior* (ed. Marumo, F.) 37–51 (Terra Sci., 1990).
5. Agee, C. B. Crystal–liquid density inversions in terrestrial and lunar magmas. *Phys. Earth Planet. Inter.* **107,** 63–74 (1998).
6. Ohtani, E. & Maeda, M. Density of basaltic melt at high pressure and stability of the melt at the base of the lower mantle. *Earth Planet. Sci. Lett.* **193,** 69–75 (2001).
7. Suzuki, A., Ohtani, E., Terasaki, H. & Funakoshi, K. Viscosity of silicate melts in $CaMgSi_2O_6$–$NaAlSi_2O_6$ system at high pressure. *Phys. Chem. Miner.* **32,** 140–145 (2005).
8. Bottinga, Y. & Weill, D. F. The viscosity of magmatic silicate liquids: A model for calculation. *Am. J. Sci.* **272,** 438–475 (1972).
9. Fujii, T. & Kushiro, I. *Yearbook* Vol. 76, 461–465 (Carnegie Inst., 1977).
10. Hirschmann, M. M. Partial melt in the oceanic low velocity zone. *Phys. Earth Planet. Inter.* **179,** 60–71 (2010).
11. Bottinga, Y. & Allègre, C. J. Partial melting under spreading ridges. *Phil. Trans. R. Soc. Lond. A* **288,** 501–524 (1978).
12. Sakamaki, T. *et al.* Measurement of hydrous peridotite magma density at high pressure using the X-ray absorption method. *Earth Planet. Sci. Lett.* **287,** 293–297 (2009).
13. Sakamaki, T. *et al.* Density of carbonated peridotite magma at high pressure using an X-ray absorption method. *Am. Mineral.* **96,** 553–557 (2011).
14. Lange, R. A. & Carmichael, I. S. E. Densities of Na_2O–K_2O–CaO–MgO–FeO–Fe_2O_3–Al_2O_3–TiO_2–SiO_2 liquids: New measurements and derived partial molar properties. *Geochim. Cosmochim. Acta* **51,** 2931–2946 (1987).
15. Funamori, N., Yamamoto, S., Yagi, T. & Kikegawa, T. Exploratory studies of silicate melt structure at high pressures and temperatures by *in situ* X-ray diffraction. *J. Geophys. Res.* **109,** 1–8 (2004).
16. Okuno, M. & Marumo, F. The structures of anorthite and albite melts. *Mineral. J.* **11,** 180–196 (1982).
17. Meade, C., Hemley, R. J. & Mao, H. K. High–pressure X-ray diffraction of SiO_2 glass. *Phys. Rev. Lett.* **69,** 1387–1390 (1992).
18. Brearley, M. & Montana, A. The effect of CO_2 on the viscosity of silicate liquids at high pressure. *Geochim. Cosmochim. Acta* **53,** 2609–2616 (1989).
19. Sobolev, A. V. & Chaussidon, M. H_2O concentration in primary melts from supra-subduction zones and mid-ocean ridges: Implications for H_2O storage and recycling in the mantle. *Earth Planet. Sci. Lett.* **137,** 45–55 (1996).
20. Dixon, J. E. & Clague, D. A. Volatiles in basaltic glasses from loihi seamount, Hawaii: Evidence for a relatively dry plume component. *J. Petrol.* **42,** 627–654 (2001).
21. Whittington, A., Richet, P. & Holtz, F. Water and the viscosity of depolymerized aluminosilicate melts. *Geochim. Cosmochim. Acta* **64,** 3725–3736 (2000).
22. Connolly, J. A. D., Schmidt, M. W., Solferino, G. & Bagdassarov, N. Permeability of asthenospheric mantle and melt extraction rates at mid-Ocean ridges. *Nature* **462,** 209–212 (2009).
23. Circone, S. & Agee, C. B. Compressibility of molten high-Ti mare glass: Evidence for crystal-liquid density inversions in the lunar mantle. *Geochim. Cosmochim. Acta* **60,** 2709–2720 (1996).
24. Spiegelman, M. Physics of melt extraction: Theory, implications and applications. *Phil. Trans. R. Soc. Lond. A* **342,** 23–41 (1993).
25. Naif, S., Key, K., Constable, S. & Evans, R. L. Melt-rich channel observed at the lithosphere–asthenosphere boundary. *Nature* **495,** 356–359 (2013).
26. Zimmerman, M. E., Zhang, S., Kohlstedt, D. L. & Karato, S. Melt distribution in mantle rocks deformed in shear. *Geophys. Res. Lett.* **26,** 1505–1508 (1999).
27. Bruhn, D., Groebner, N. & Kohlstedt, D. L. An interconnected network of core–forming melts produced by shear deformation. *Nature* **403,** 883–886 (2000).
28. Hier–Majumder, S. Development of anisotropic mobility during two–phase flow. *Geophys. J. Int.* **186,** 59–68 (2011).
29. Karato, S. On the origin of the asthenosphere. *Earth Planet. Sci. Lett.* **321–322,** 95–103 (2012).
30. Lewis, J., Schwarzenbach, D. & Flack, H. D. Electric field gradients and charge density in corundum, α–Al_2O_3. *Acta Crystallogr A* **38,** 733–739 (1982).

Acknowledgements

This work was supported by Grant-in-Aid awards for Scientific Research to E.O. (numbers 16340164, 18104009 and 22000002) and S.U. (numbers 13440163, 16340170 and 20103003) from the Ministry of Education, Culture, Sports, Science, and Technology of the Japanese Government. This work was also partially supported by the Global Center of Excellence program of Earth and Planetary Science, Tohoku University, Japan. T.S. was supported by a Research Fellowship of the Japan Society for the Promotion of Science for Young Scientists. The synchrotron radiation experiments were performed at SPring-8 with the approval of the Japan Synchrotron Radiation Research Institute (Proposal No. 2004A0250, 2004B0049, 2005A0453, 2005B0011, 2006A3705, 2006B3710, 2002B0087, 2003A0057, 2003B0036, 2004A0384, 2004B0646, 2007A1095 and 2009A1661) and Japan Atomic Energy Agency (Proposal No. 2002-S-01, 2003-S-05, 2004-S-04, 2006A-E17 and 2006B-E23). Y.W. acknowledges support from the NSF (EAR 0711057). All authors acknowledge useful discussions with and suggestions by S. Labrosse.

Author contributions

T.S., S.U., A.S., E.O. and Y.K. performed the density measurements. A.S., H.T., E.O., T.S. and K-i.F. carried out the viscosity measurements. T.S., A.S., H.T., E.O. and K-i.F. performed the structure measurements. T.S., E.O., A.S., Y.W. M.D.B. and J.W.H. made arguments on geological applications of the experimental results, and prepared the paper. All authors discussed the results and commented on the manuscript.

Additional information

Supplementary information is available in the online version of the paper. Reprints and permissions information is available online at www.nature.com/reprints. Correspondence and requests for materials should be addressed to T.S.

Competing financial interests

The authors declare no competing financial interests.